MRS Communications

https://doi.org/10.1557/s43579-022-00219-z

MRS Communications

Early Career Materials Researcher Research Letter

Fabrication of physically crosslinked lignin–PVA hydrogels containing high concentrations of fractionated and cleaned lignins

Keturah Bethel, Annie Buck, Graham Tindall, Mark C. Thies, Eric M. Davis, Department of Chemical and Biomolecular Engineering, Clemson University, Clemson, SC 29631, USA

Address all correspondence to Eric M. Davis at **ericd@clemson.edu**

(Received 11 May 2022; accepted 21 July 2022)

Abstract

Herein, two series of lignin–poly(vinyl alcohol) (PVA) composite hydrogels were fabricated, using both Kraft lignin (raw, unfractionated lignin) and ultraclean lignin (fractionated lignin of controlled molecular weights). These hydrogels were synthesized via the freeze–thaw method, whereby physical crosslinks between PVA chains were created. Specifically, the lignin concentration and molecular weight were systematically varied, ranging from lignin molecular weights of ≈5700 g mol^{-1} to ≈160,000 g mol^{-1} at lignin concentrations of 20 wt% to 60 wt%. Results indicate that both the lignin concentration and molecular weight, as well as the number of freeze–thaw cycles, directly influence both the water uptake and the network structure of these soft composites.

As efforts to reduce consumption of fossil fuels continue to rise, there is an increasing need to produce "greener" or more sustainable materials.[1,2] To address this issue, the synthesis of renewable soft composites using alginate, cellulose, and lignin has been heavily explored.[1–4] There has been significant progress over the last decade with regards to the use of lignin as a macromolecular building block for greener soft composites, owing to the ample hydroxyl and carbonyl groups within its structure, which provide avenues for chemical functionality and subsequently, enhanced technologies.[2,5] Lignin is also an attractive building block for advanced materials due to its relative abundance and the potential to add economic value to materials fabrication, as currently over 99% of the ≈ 50 million tons of lignin produced annually are simply burned as fuel.[6,7] In addition, lignin is the only naturally occurring source of phenolic compounds,[5,6] making it attractive for membrane-based protein separation technologies.[8,9]

However, traditional Kraft lignin is impure and has a broad range of molecular weights (MWs), leading to variability in the chemical functionality. Previous work in this area has explored the fabrication of lignin-based hydrogels through both chemical[7] and physical crosslinking,[10–12] though the latter fabrication route has received far less attention. Physically crosslinked lignin-based hydrogels are attractive, given that they do not require the presence of harsh chemical additives such as crosslinkers and initiators since the formation of the dense membrane network structure is governed by intermolecular forces or entanglements of polymer chains.[12–15] The absence of such additives in physically crosslinked soft composites uniquely qualifies this class of materials for delicate applications, including drug delivery and tissue scaffolding.[3,10,14,15]

Physically crosslinked hydrogels are commonly created by the "freeze–thaw method",[12,16–18] whereby a free-standing membrane is formed by sequentially freezing and then thawing a polymer solution. In the case of PVA, the freeze–thaw cycles create ordered regions that crystallize and remain intact once thawed, due to the intermolecular forces of the hydroxyl groups. These crystalline regions serve as the crosslink junctions for the three dimensional crosslinked network.[11,12] Upon increasing the number of freeze–thaw cycles, the crystalline domains strengthen or further densify, often resulting in a more ordered, uniform network structure.[11] Previous research efforts have focused on expanding the field of bio-based, physically-crosslinked hydrogels through the incorportation of hemicellulose and chitosan.[16,19,20] However, lignin remains an underexplored resource for such purposes, given the limited number of studies on these physically crosslinked materials in the literature. In one of the few investigations on these materials, Morales and coworkers[10,18,21] investigated the impact of processing parameters, such as the source of the lignin, number of freeze–thaw cycles, and lignin concentration, on the transport and mechanical properties of the resulting hydrogels. While their results demonstrated a clear influence of lignin on the transport and mechanical properties,[10,21] only a single lignin molecular weight was investigated.

Similarly, investigators recently fabricated lignin–chitosan–PVA soft composites, for wound dressing, using a single lignin molecular weight via the freeze–thaw method. These soft composites exhibited improved mechanical properties and adsorption capacity when compared to the neat PVA hydrogels, highlighting the improved performance achieved through the introduction of these biopolymers.[22] However, due to the heterogenous and complex nature of the unfractionated lignin

utilized in these studies,[3,7] the development of fundamental structure–processing–property relationships of these lignin-based physically crosslinked soft composites remains hindered. Further, as these investigations only characterized PVA–lignin composites at a single-lignin MW, the impact of lignin MW on the property of these physically crosslinked soft composites remains uknown.

Other notable recent work includes the fabrication of nanolignin-filled PVA hydrogels with improved conductive properties, as well as the fabrication of lignin-containing cellulose nanocrystals, doped in bentonite, with improved absorption rates of organic dyes.[23,24] While these studies resulted in lignin-containing soft composites with improved performance properties, the molecular weight of the lignin used was not specified, limiting our ability to develop relationships between lignin molecular weight and the final hydrogel properties. To address this issue, a novel lignin purification approach, known as the aqueous lignin purification with hot agents (ALPHA) process,[6,25] which provides the ability to simultaneously fractionate and clean Kraft lignins, was employed. With access to purified lignins of prescribed molecular weights, we are uniquely positioned to more directly probe the structure-processing-property relationships in this emerging class of green materials. With the ability to directly manipulate the network structure of these hydrogels via lignin molecular weight, soft composites with tailored transport and mechanical properties[26,27] can be synthesized for a wide range of applications, including membrane-baseed water filtration and purification, as well as lignin-based soft composites for tissue engineering.

In this work, two series of physically crosslinked lignin-PVA composite hydrogels were fabricated via the freeze–thaw method ranging from one (1×) to three (3×) freeze–thaw cycles. Three different lignin fractions were utilized: (1) unfractionated Kraft lignin [referred to as BioChoice™ lignin (BCL)]; (2) low MW (LMW), ultra clean lignin; and (3) high MW (HMW), ultra clean lignin, where the latter two lignin fractions were obtained by simultaneously fractionating and cleaning Kraft lignin via the ALPHA process. Within each series of soft composites, the hydrogels were synthesized with lignin contents of 20 wt% and 60 wt%. To our knowledge, this is the highest lignin concentration implemented in the fabrication of this class of physically crosslinked hydrogel composites. Note, an illustrative schematic of the hydrogel synthesis procedure, along with images of the dense, free-standing composites obtained, are shown in Figure S1 in the Supplementary Information (SI). After fabrication, the impact of lignin concentration and number of freeze–thaw cycles on the hydrophobicity of each soft composite was characterized by measuring the equilibrium water uptake of each membrane. Additionally, the swollen network structure of each soft composite was directly imaged via scanning electron microscopy (SEM).

Table I summarizes the synthesis conditions for the three series of lignin-PVA soft composites, as well as the specific nomenclature that will be used to represent the various membranes moving forward.

For example, 10–LMW–60–3× will be used to represent lignin–PVA hydrogels that were fabricated using a 10 wt% PVA solution containing 60 wt% LMW lignin, which was subjected to three freeze–thaw cycles to form the final

Table I. Nomenclature for neat PVA and lignin–PVA soft composites synthesized via the freeze–thaw method.

Lignin fraction	Lignin content[b]	PVA concentration in DMSO solution (wt%)	No. freeze–thaw cycles	Nomenclature
Neat PVA (no lignin)	N/A	5	1	5–Neat–1×
			3	5–Neat–3×
	N/A	10	1	10–Neat–1×
			3	10–Neat–3×
BioChoice™[a] (BCL)	20 wt%	5	1	5–BCL–20–1×
			3	5–BCL–60–1×
	60 wt%	10	1	10–BCL–60–3×
			3	10–BCL–60–3×
Low MW (LMW)	20 wt%	5	1	5–LMW–20–1×
			3	5–LMW–20–3×
	60 wt%	10	1	10–LMW–60–1×
			3	10–LMW–60–3×
High MW (HMW)	20 wt%	5	1	5–HMW–20–1×
			3	5–HMW–20–3×
	60 wt%	10	1	10–HMW–60–1×
			3	10–HMW–60–3×

[a]BioChoice is the trademarked name of the feed/raw lignin, which is then subjected to fractionation and cleaning by the ALPHA process to produce the low MW and high MW lignin fractions.

[b]The concentrations of the various lignin fractions are based on the total mass of solids in solution. Here, the total mass of solids is equal to the mass of lignin + mass of PVA in the DMSO solution.

soft composite. Note that the PVA concentration is given based on the PVA–DMSO solution, while the lignin concentration is given based on the total mass of polymer, i.e., $m_{\text{lignin}}/(m_{\text{PVA}} + m_{\text{lignin}})$. Figure 1 shows the equilibrium water uptake data for both neat PVA, as well as lignin–PVA soft composites. Specifically, the equilibrium water uptake of soft composites fabricated at various lignin concentrations using 5 wt% and 10 wt% PVA–DMSO solutions are shown in Fig. 1(a) and (b), respectively. Note, in Fig. 1, membranes that have undergone 1 × and 3 × freeze–thaw cycles are shown in solid blue bars and shaded red bars, respectively. Focusing our attention on 1 × freeze–thaw samples fabricated from a 5 wt% PVA–DMSO solution [solid blue bars in Fig. 1(a)], we note that there is little variation in the equilibrium water uptake with the introduction of 20 wt% lignin apart from 5–BCL–20–1 ×, where an approximate twofold increase in water uptake is observed when compared to 5–Neat–1 ×. Specifically, the equilibrium water uptake is seen to increase from 883% ± 200% to 1455% ± 12%. Given that the lignin added into the system is relatively hydrophobic, this result is quite surprising and unexpected. When the BCL concentration is increased from 20 to 60 wt%, the water uptake of 5–BCL–60–1 × decreased to 683% ± 40%, which is less than half that of 5–BCL–20–1 ×, as well as ≈ 20% lower than that of 5–Neat–1 ×. This result is more in line with what we would expect when replacing more than half of the hydrophilic PVA with the more hydrophobic lignin.

Next, examining the 3 × freeze–thaw membranes [shaded red bars in Fig. 1(a)], we first observe that the water uptake of neat PVA decreases by ≈ 30 wt% with an increase in the number of freeze–thaw cycles. As mentioned earlier, this behavior is expected as the PVA crystalline structure, and subsequently the crosslinked network, is reinforced with each freeze cycle,[11,12] leading to a decrease in the mesh size and equilibrium water uptake for these membranes. Interestingly, this behavior is different than recent results from Morales et al.,[21] who observed little change in the swelling kinetics and degree of swelling for neat PVA hydrogels as a function of the number of freeze–thaw cycles. This discrepancy may be attributed to the difference in freeze times, where hydrogels in that study were only subjected to 2 h of freezing, while hydrogels in this study were frozen for 24 h.

Surprisingly, this subsequent decrease in equilibrium water uptake with increasing number of freeze–thaw cycles was only observed for soft composites containing BCL. For example, increasing the number of freeze–thaw cycles from 1 × to 3 × results in a reduction of the water uptake by approximately half when comparing 5–BCL–20–1 × to 5–BCL–20–3 ×. However, when compared to 5–Neat–3 ×, it is not until the BCL concentration reaches 60 wt% that we observe a statistically significant decrease in water uptake, going from a value of 610% ± 20% for 5–Neat–3 × to a value of 455% ± 60% for 5–BCL–60–3 ×. In contrast to hydrogels containing BCL, a statistically significant increase in the equilibrium water uptake is observed with the introduction of both LMW and HMW lignin. Specifically, the equilibrium water uptake is seen to increase to 898% ± 22% and 845% ± 85% for 5–LMW–20–3 × and 5–HMW–20–3 ×, respectively. Further, while a decrease in water uptake is observed when the LMW lignin content is increased to 60 wt%, little variation in water uptake is observed among 5–LMW–60–3 ×, 5–HMW–20–3 ×, and 5–HMW–60–3 ×, which all exhibited water uptake values of ≈ 800%. It is also interesting to note that at a specific LMW and HMW lignin fraction and content, the equilibrium water uptake does not change appreciably with an increase from 1 × to 3 × freeze–thaw cycles. That is, there are no statistically significant differences between the solid blue and shaded red bars

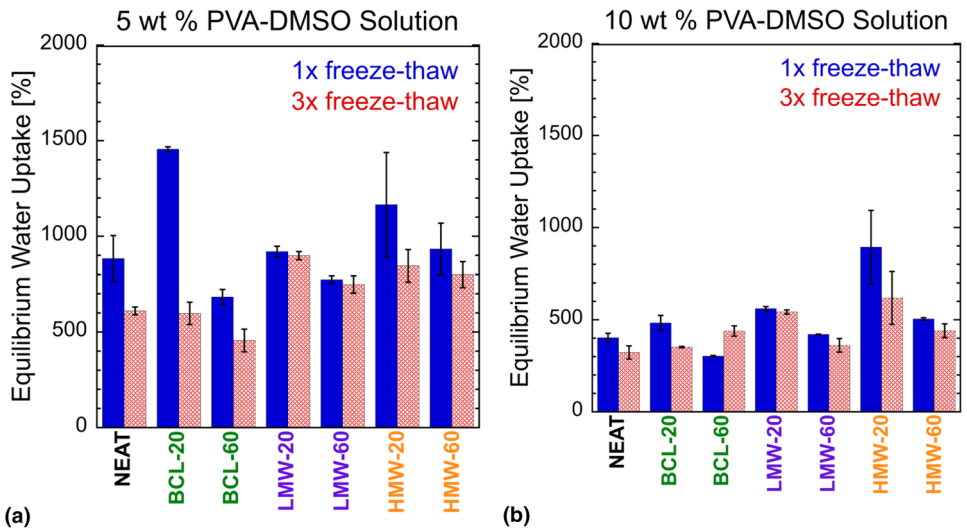

Figure 1. Equilibrium water uptake of neat PVA and lignin–PVA soft composites fabricated from PVA–DMSO solutions containing (a) 5 wt% and (b) 10 wt% PVA. Note, the solid blue and shaded red bars represent equilibrium water uptake values for membranes that have undergone one (1 ×) and three (3 ×) freeze–thaw cycles, respectively. The error bars represent the standard deviation of the average, which was calculated from at least three repeat experiments on separate membranes.

for these soft composites in Fig. 1(a). It is not clear why the equilibrium water uptake behavior of these samples is different from their BCL-containing counterparts, though we suspect this may be related to the wide range of MWs present in the BCL fraction, making the impact of this lignin fraction on the final properties of the soft composites less predictable. Further, given that the ALPHA process simultaneously fractionates and cleans the BCL, this difference may be also be a result of the higher impurities (i.e., higher ash content) present in this lignin prior to fractionation.

Next, focusing our attention on 1 × freeze–thaw samples fabricated from a 10 wt% PVA-DMSO solution [solid blue bars in Fig. 1(b)], we note that the equilibrium water uptake values in this series of soft composites are generally lower than that of their 5 wt% PVA counterparts [Fig. 1(a) vs. (b)]. The only exception to this is 10–HMW–20–1 ×, which has a similar equilibrium water uptake to that of 5–HMW–20–1 ×. The observed decrease in equilibrium water uptake is a result of the increased concentration of PVA in the PVA–DMSO solution used to fabricate the physically crosslinked hydrogels. As the concentration of PVA is increased, there is an increase in hydrogen bonding between PVA chains, resulting in the creation of more crystalline domains and a higher degree of crosslinking.[13] Interestingly, for all lignin fractions, we observe an initial increase in equilibrium water uptake with the introduction of lignin at a concentration of 20 wt%. Notably, the highest increase in equilibrium water uptake was observed for 10–HMW–20–1 ×, where the water uptake was measured to be 893% ± 199%, an approximate 150% increase from 10–Neat–1 ×. This result is consistent with work by Morales et al.,[21] where an increase in both the swelling rate and degree of swelling, compared to neat PVA, was observed for samples containing lignin compared to neat PVA. The increase in water uptake with the introduction of 20 wt% lignin may be a result of the lignin disrupting the formation of the physically crosslinked PVA network formed during freeze–thaw cycles of the PVA–DMSO solution.

As the lignin does not participate in the formation of the crosslinked network formed during sequential freeze–thaw cycles, the lignin chains have the potential to block the intermolecular forces (i.e., hydrogen bonding) between PVA chains that facilitate PVA crystallization or crystallite formation, which serve as crosslink junctions during the freeze–thaw process.[12,13,26] This 'blocking' of the PVA chains may be due to the steric hindrance of the lignin phase, or it may be a result of the lignin hydrogen bonding with the PVA,[28] preventing the PVA from hydrogen bonding with itself. In either case, this will result in a lower degree of physical crosslinking and larger mesh sizes,[26] ultimately allowing for higher water absorption for these soft composites. Similar to what was observed for the 1 × 5 wt% PVA hydrogels, when the lignin concentration is increased to 60 wt%, we observe that for a particular lignin fraction the equilibrium water uptake decreases [e.g., see 10–BCL–20–1 × vs. 10–BCL–60–1 × in Fig. 1(b)]. At 60 wt%, it appears that the relative hydrophobicity of the lignin begins to govern the hydrophilicity of the soft composites. That is, the hydrophobicity of the lignin counteracts the impact lignin has on disrupting the PVA network formation.

Next, focusing our attention on the 3 × samples [shaded red bars in Fig. 1(b)], we observe that the equilibrium water uptake generally increases with the introduction of lignin, apart from 10–BCL–20–3 × and 10–LMW–60–3 ×, which demonstrated no statistically significant change in water uptake from that of 10–Neat–3 ×. Interestingly, when the BCL concentration was increased from 20 to 60 wt%, an increase of ≈ 30% in water uptake was observed. However, consistent with the trend we observed for the 1 × freeze–thaw composites [solid blue bars in Fig. 1(b)], when the LMW and HMW lignin content was increased to 60 wt%, a decrease in water uptake was observed. Again, we believe this is related to the hydrophobicity of the lignin, which counteracts the impact lignin has on disrupting the PVA network formation.

When comparing the general trends observed between the two series of soft composites [i.e., Fig. 1(a) vs. (b)], we observe an increase in water uptake when lignin was introduced at 20 wt% into the 10 wt% PVA soft composites, which is not observed for the 5 wt% PVA soft composites. We believe this is related to the lowered probability of the lignin interacting with PVA chains when the concentration of PVA is reduced by half. As mentioned above, this result suggests that the presence of lignin (at least at a content of 20 wt%) is impeding the formation of physical PVA crosslink junctions, resulting in a looser crosslinked network structure. These larger mesh sizes lead to increased water uptake (i.e., hydrophilicity) for these soft composites, as the lower concentration of crosslink junctions more easily facilitates water-induced swelling of the hydrogel.[26,27] Moreover, the hydrogels in each series generally demonstrated a reduction in the water uptake when the lignin concentration was increased to 60 wt%. This is not surprising as the lignin itself is more hydrophobic relative to the PVA it is replacing.[13] In summary, we posit that at a lignin content of 20 wt%, the lignin generally acts to impede the PVA crosslinking, leading to similar or higher equilibrium water uptake values to that of neat PVA, while at a lignin content of 60 wt%, the hydrophobicity of the lignin more significantly impacts the water uptake behavior of the soft composites (i.e., the hydrophobicity of the lignin counteracts its disruptive effect on PVA network formation).

To determine the impact of the various lignin fractions, as well as the impact of lignin concentration on the hydrated network structure of the soft composites, the surface morphology of the hydrogels was characterized using scanning electron microscopy (SEM). Images of the hydrated network structure of soft composites fabricated from a 5 wt% PVA–DMSO solution are shown in Fig. 2. Specifically, images of the network structure of soft composites that have undergone 1 × and 3 × freeze–thaw cycles are shown in Fig. 2(a) and (b), respectively. Note that additional SEM images at a lower magnification can be found in Figs. S2 and S3 in the SI. Comparing 5–Neat–1 × to its lignin-containing counterparts [Fig. 2(a)], we see that the addition of BCL resulted in a network structure that is much less defined with larger pores, with the presence

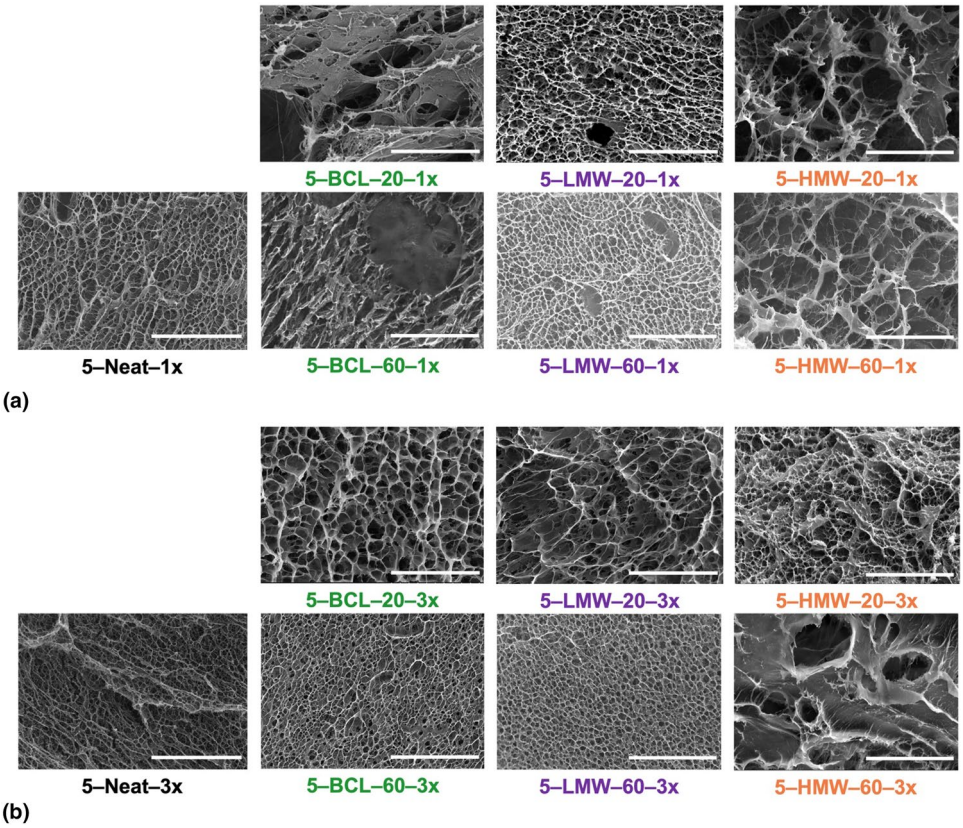

Figure 2. Scanning electron microscopy (SEM) images of hydrated neat PVA and lignin–PVA soft composites, fabricated from a 5 wt% PVA–DMSO solution, that have undergone (a) one (1 ×) and (b) three (3 ×) freeze–thaw cycles. Note, the various fractions of lignin have been organized in columns, while the lignin concentrations of 20 wt% and 60 wt% have been organized in rows. Specific labels, following the nomenclature listed in Table I, are provided below each SEM image. Also note, the scale bar in all the images is 20 μm.

of large lignin aggregates in the hydrogel. Surprisingly, as the BCL concentration is increased to 60 wt%, we observe the presence of a more uniform network, though we still observe large agglomerations of lignin (≈ 20 μm in diameter) within the membrane, as seen by the darker shaded globules. The improved network structure of 5–BCL–60–1 × directly correlates to the observed reduction in water uptake of these membranes when compared to 5–BCL–20–1 ×.

In contrast, the addition of LMW lignin did not significantly impact the resulting network structure. As seen in the image for 5–LMW–20–1 ×, the network structure is similar to that of 5–Neat–1 ×. When the LMW lignin concentration is increased to 60 wt%, we observe that, on average, the size of the pores in the membrane are smaller than those of its 20 wt% counterpart (i.e., 5–LMW–20–1 × vs. 5–LMW–60–1 ×). These direct images of the hydrated network structure correlate nicely with differences (or lack thereof) observed in the equilibrium water uptake among these hydrogels [see Fig. 1(a)]. That is, the equilibrium water uptake of 5–LMW–20–1 × and 5–Neat–1 × are statistically similar, while 5–LMW–20–1 × exhibits higher water uptake (i.e., is more hydrophilic) than 5–LMW–60–1 ×. Similar to soft composites containing BCL, a large disruption of the network structure with the introduction of HMW lignin was observed for both 5–HMW–20–1 × and 5–HMW–60–1 ×. Specifically, the network structures of these soft composites were relatively heterogenous, exhibiting large variations in the pore size, similar to what is seen for 5–BCL–20–1 ×. This heterogeneity in network structure is manifested in the high variability in the measured water uptake between individual membranes [i.e., manifested as large error bars in Fig. 1(a)]. The network structure captured in the SEM images for 5–HMW–20–1 × and 5–HMW–60–1 × are similar, which coincides with the statistically similar values of equilibrium water uptake measured for each membrane. In general, the SEM images shown in Fig. 2(a) support the observed differences in water uptake (i.e., hydrophilicity) among the various soft composites shown by the solid blue bars in Fig. 1(a).

Next, focusing our attention on the SEM images shown in Fig. 2(b), we observe a tightening of the network structure for neat PVA and composites containing BCL [first two columns in Fig. 2(b)] when the number of freeze–thaw cycles was increased from 1 × to 3 ×. There is, in general, a tightening of the network structure, though this is most obvious in SEM images of 5–BCL–60–3 × and 5–LMW–60–3 × [middle two images on bottom row of Fig. 2(b)]. Further, apart from composites containing HMW lignin, a tighter network structure is observed

when the lignin concentration is increased from 20 to 60 wt% [top row vs. bottom row in Fig. 2(b)]. This tightening of the network structure corroborates the reduction in equilibrium water uptake observed for 5–BCL–60–3 × and 5–LMW–60–3 × when compared to their 20 wt% counterparts [comparing shaded red bars in Fig. 1(a)]. However, this tightening in network structure was not observed for all 3 × freeze–thaw soft composites. Specifically, an increase in the hydrated pore size was observed for 5–LMW–20–3 ×, which is reflected in the higher water uptake for these membranes when compared to 5–Neat–3 ×. Additionally, the similar equilibrium water uptake measured for 5–LMW–20–1 × and 5–LMW–20–3 × can be explained by the similar network structure seen in the SEM images of these membranes in Fig. 2(a) and (b).

Moving our attention now to hydrogels fabricated using a 10 wt% PVA-DMSO solution, Fig. 3(a) and (b) show the SEM images for membranes that have been subjected to 1 × and 3 × freeze–thaw cycles, respectively. Notably, much smaller pore sizes are observed in the network structures when compared to their 5 wt% PVA counterparts. Specifically, 10–Neat–1 × appears to not only have smaller pore sizes than 5–Neat–1 ×, but images of these soft composites indicate larger portions of a 'less disrupted' PVA phase, as shown by the flat, grey regions in the SEM image. For the 1 × samples, when lignin is first introduced into the hydrogel network structure, there is a slight increase in the pore size and an increased frequency of lignin agglomerates, apart from 10–HMW–20–1 ×. The 10–HMW–20–1 × sample appeared to have a more uniform, tighter network structure with relatively smaller pores than its neat counterpart. However, the PVA phase in these images is 'more disrupted'—i.e., the concentration of PVA in the image is lower than that in the image of 10–Neat–1 ×. This may help explain why the water uptake for 10–HMW–20–1 × is over two-fold higher than 10–Neat–1 ×. That is, while, on average, the pores of 10–Neat–1 × are larger, there is a greater degree of water uptake by 10–HMW–20–1 × due to the higher concentration of 'water-rich' region in these membranes. Further, this discrepancy may be related to the heterogeneous nature of the HMW samples, also indicated by the high variation of the water uptake between individual sample, similar to what was demonstrated by the 5 wt% PVA counterparts [see Fig. 1(a) and (b)]. While the area that is captured shows the morphology mentioned above, it is suspected that there are local domains with varying morphologies within the network structure of this sample.

As the lignin concentration increased to 60 wt%, the network structure appeared to tighten for all lignin molecular weights. This is most easily seen in the SEM images of

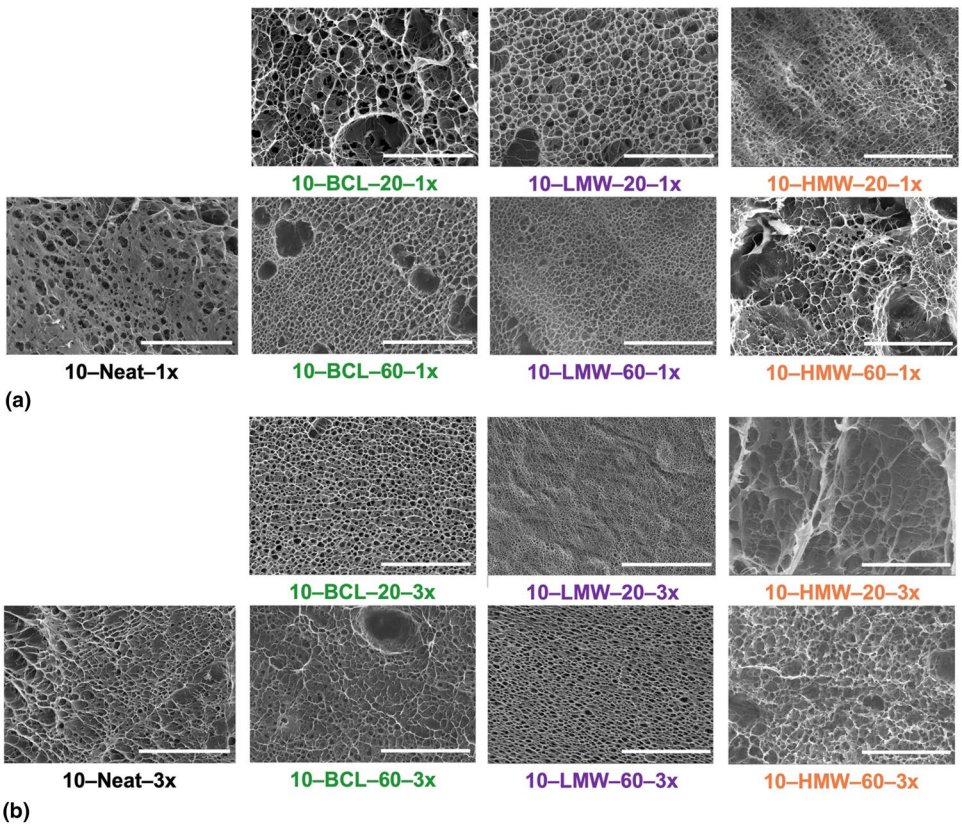

Figure 3. Scanning electron microscopy (SEM) images of hydrated neat PVA and lignin–PVA soft composites, fabricated from a 10 wt% PVA-DMSO solution, that have undergone (a) one (1 ×) and (b) three (3 ×) freeze–thaw cycles. Note, the various fractions of lignin have been organized in columns, while the lignin concentrations of 20 wt% and 60 wt% have been organized in rows. Specific labels, following the nomenclature listed in Table I, are provided below each SEM image. Also note, the scale bar in all the images is 20 μm.

10–BCL–60–1 × and 10–LMW–60–1 × [two middle images in bottom row of Fig. 3(a)]. The reduction in pore size with the addition of lignin is mirror in the water uptake data for these samples, where all 1 × soft composites with 60 wt% lignin (irrespective of the lignin molecular weight) showed a statistically significant decrease in equilibrium water uptake [see solid blue bars in Fig. 1(b)]. As the number of freeze–thaw cycles was increased from 1 × to 3 ×, the network structure visually appeared to tighten and smaller pore sizes are observed, though this difference is not as pronounced in soft composites containing LMW lignin. The similar network structure caputure in the SEM images of hydrogels containing LWM lignin helps to explain why no statistically significant difference in water uptake is observed for these membranes when the number of freeze–thaw cycles is increased [compare solid blue bars and shaded red bars in Fig. 1(b)]. Interestingly, only the 10–Neat–3 × and 10–BCL–20–3 × showed a decrease in water uptake. The increase in water uptake for 10–BCL–60–3 ×, when compared to 10–BCL–60–1 ×, may be related to the lower frequency of BCL agglomerates in the SEM images for this material, allowing for a more uniform network structure for 10–BCL–60–3 ×.

In conclusion, we have demonstrated the successful fabrication of dense, free-standing lignin-PVA soft composites, with lignin concentrations as high as 60 wt%, via the freeze–thaw method. These hydrogel composites were fabricated using both raw, unfractionated Kraft lignin, as well as lignin that had been fractionated and cleaned by the ALPHA process. It is clear from both the water uptake data and the SEM images that the lignin concentration, as well as the lignin molecular weight can be leveraged to influence the network structure of these soft composites. In general, the addition of lignin at a concentration of 20 wt% resulted in an increase in equilibrium water uptake for all samples, irrespective of the PVA wt% and number of freeze–thaw cycles the membranes had undergone. When the lignin concentration was increased to 60 wt%, the water uptake was seen to decrease relative to the 20 wt% counterparts. The number of freeze–thaw cycles was seen to have little impact on the water uptake and network structure of soft composites containing LMW and HMW lignin. For the former, this can be attributed to the more uniform crosslinked network that was created in these membranes, where it appears that the LMW lignin was more easily uniformly distributed throughout the PVA matrix, as evidenced by the low frequency of lignin aggregates. This result highlights that we can create soft composites with a high concentration of a renewable biopolymer while not significantly impacting the hydrophilicity of the resulting membrane. On the other hand, we believe that the heterogeneous network structure created in HMW lignin membranes, particularly those formed from a 5 wt% PVA–DMSO solution, serves to mask the impact of the number of freeze–thaw cycles, which can be seen in the large error bars in the water uptake data for these membranes. Our results underscore the benefits of the ALPHA process, whereby the molecular weight of the lignin, as well as the lignin purity, can be controlled and utilized to directly manipulate the soft composite network structure. We believe that the results from this work provide a framework for the fabrication of sustainable soft composites with tailored hydrophilicty by providing a set of processing–property relationships for physically crosslinked lignin-based hydrogels.

Acknowledgments

The authors would like to acknowledge the generous support from the National Science Foundation (NSF) (Grant No. CBET-1915787). Both Keturah Bethel and Graham Tindall would like to also acknowledge the generous support of the Department of Education Graduate Assistance in Areas of National Need (GAANN) Fellowship (Award No. P200A180076). The authors would also like to acknowledge financial support from the Clemson University's Creative Inquiry Program.

Author contributions

KB: formal analysis, investigation, writing—original draft, visualization. AB: investigation, writing—review & editing. GT: investigation, writing—review & editing. MCT: writing—review & editing. EMD: conceptualization, validation, writing—review & editing, supervision.

Data availability

The datasets generated during and/or analyzed during the current study are available from the corresponding author on reasonable request.

Declarations

Conflict of interest

The authors declare no competing financial interest.

Supplementary Information

The online version contains supplementary material available at https://doi.org/10.1557/s43579-022-00219-z.

References

1. Y. Meng, J. Lu, Y. Cheng, Q. Li, H. Wang, Lignin-based hydrogels: a review of preparation, properties, and application. Int. J. Biol. Macromol. **135**, 1006–1019 (2019). https://doi.org/10.1016/j.ijbiomac.2019.05.198
2. G.W. Tindall, J. Chong, E. Miyasato, M.C. Thies, Fractionating and purifying softwood kraft lignin with aqueous renewable solvents: liquid–liquid equilibrium for the lignin–ethanol–water system. Chemsuschem **13**(17), 4587–4594 (2020). https://doi.org/10.1002/cssc.202000701
3. W. Yang, E. Fortunati, F. Bertoglio, J.S. Owczarek, G. Bruni, M. Kozanecki, J.M. Kenny, L. Torre, L. Visai, D. Puglia, Polyvinyl alcohol/chitosan hydrogels with enhanced antioxidant and antibacterial properties induced by lignin nanoparticles. Carbohydr. Polym. **181**, 275–284 (2018). https://doi.org/10.1016/j.carbpol.2017.10.084

4. L. Jin, R. Bai, Mechanisms of lead adsorption on chitosan/PVA hydrogel beads. Langmuir **18**(25), 9765–9770 (2002). https://doi.org/10.1021/la025917l
5. Klett, A. S. Purification, fractionation, and characterization of lignin from kraft black liquor for use as a renewable biomaterial. 174.
6. A.S. Klett, P.V. Chappell, M.C. Thies, Recovering ultraclean lignins of controlled molecular weight from kraft black-liquor lignins. Chem. Commun. **51**(64), 12855–12858 (2015). https://doi.org/10.1039/C5CC05341B
7. N. Gregorich, J. Ding, M.C. Thies, E.M. Davis, Novel composite hydrogels containing fractionated, purified lignins for aqueous-based separations. J. Mater. Chem. A (2021). https://doi.org/10.1039/D0TA09046H
8. D. Karefyllakis, S. Altunkaya, C.C. Berton-Carabin, A.J. van der Goot, C.V. Nikiforidis, Physical bonding between sunflower proteins and phenols: impact on interfacial properties. Food Hydrocoll. **73**, 326–334 (2017). https://doi.org/10.1016/j.foodhyd.2017.07.018
9. J. Kroll, H.M. Rawel, Reactions of plant phenols with myoglobin: influence of chemical structure of the phenolic compounds. J. Food Sci. **66**(1), 48–58 (2001). https://doi.org/10.1111/j.1365-2621.2001.tb15580.x
10. A. Morales, J. Labidi, P. Gullón, Assessment of green approaches for the synthesis of physically crosslinked lignin hydrogels. J. Ind. Eng. Chem. **81**, 475–487 (2020). https://doi.org/10.1016/j.jiec.2019.09.037
11. J. Tavakoli, J. Gascooke, N. Xie, B.Z. Tang, Y. Tang, Enlightening freeze-thaw process of physically cross-linked poly(vinyl alcohol) hydrogels by aggregation-induced emission fluorogens. ACS Appl. Polym. Mater. **1**(6), 1390–1398 (2019). https://doi.org/10.1021/acsapm.9b00173
12. S.R. Stauffer, N.A. Peppast, Poly(vinyl alcohol) hydrogels prepared by freezing-thawing cyclic processing. Polymer **33**(18), 3932–3936 (1992). https://doi.org/10.1016/0032-3861(92)90385-A
13. Structure and Application of PVA Hydrogels Peppas.Pdf.
14. E.M. Ahmed, Hydrogel: preparation, characterization, and applications: a review. J. Adv. Res. **6**(2), 105–121 (2015). https://doi.org/10.1016/j.jare.2013.07.006
15. Y.-H. Tsou, J. Khoneisser, P.-C. Huang, X. Xu, Hydrogel as a bioactive material to regulate stem cell fate. Bioact. Mater. **1**(1), 39–55 (2016). https://doi.org/10.1016/j.bioactmat.2016.05.001
16. M.D. Figueroa-Pizano, I. Vélaz, M.E. Martínez-Barbosa, A freeze-thawing method to prepare chitosan-poly(vinyl alcohol) hydrogels without crosslinking agents and diflunisal release studies. JoVE J. Vis. Exp. **155**, e59636 (2020). https://doi.org/10.3791/59636
17. J.I. Daza Agudelo, J.M. Badano, I. Rintoul, Kinetics and thermodynamics of swelling and dissolution of PVA gels obtained by freeze-thaw technique. Mater. Chem. Phys. **216**, 14–21 (2018). https://doi.org/10.1016/j.matchemphys.2018.05.038
18. A. Morales, J. Labidi, P. Gullón, Impact of the lignin type and source on the characteristics of physical lignin hydrogels. Sustain. Mater. Technol. **31**, e00369 (2022). https://doi.org/10.1016/j.susmat.2021.e00369
19. Y. Guan, B. Zhang, J. Bian, F. Peng, R.-C. Sun, Nanoreinforced hemicellulose-based hydrogels prepared by freeze-thaw treatment. Cellulose **21**(3), 1709–1721 (2014). https://doi.org/10.1007/s10570-014-0211-9
20. Y. Guan, J. Bian, F. Peng, X.-M. Zhang, R.-C. Sun, High strength of hemicelluloses based hydrogels by freeze/thaw technique. Carbohydr. Polym. **101**, 272–280 (2014). https://doi.org/10.1016/j.carbpol.2013.08.085
21. A. Morales, J. Labidi, P. Gullón, Effect of the formulation parameters on the absorption capacity of smart lignin-hydrogels. Eur. Polym. J. **129**, 109631 (2020). https://doi.org/10.1016/j.eurpolymj.2020.109631
22. Y. Zhang, M. Jiang, Y. Zhang, Q. Cao, X. Wang, Y. Han, G. Sun, Y. Li, J. Zhou, Novel lignin–chitosan–PVA composite hydrogel for wound dressing. Mater. Sci. Eng. C **104**, 110002 (2019). https://doi.org/10.1016/j.msec.2019.110002
23. Y. Wang, S. Liu, Q. Wang, X. Ji, X. An, H. Liu, Y. Ni, Nanolignin filled conductive hydrogel with improved mechanical, anti-freezing, UV-shielding and transparent properties for strain sensing application. Int. J. Biol. Macromol. **205**, 442–451 (2022). https://doi.org/10.1016/j.ijbiomac.2022.02.088
24. M. Jiang, N. Niu, L. Chen, A template synthesized strategy on bentonite-doped lignin hydrogel spheres for organic dyes removal. Sep. Purif. Technol. **285**, 120376 (2022). https://doi.org/10.1016/j.seppur.2021.120376
25. Thies, M.C., Klett, A.S, Bruce, D.A. Solvent and recovery process for lignin. US10053482 B2, 2015.
26. A.S. Hickey, N.A. Peppas, Mesh size and diffusive characteristics of semicrystalline poly(vinyl alcohol) membranes prepared by freezing/thawing techniques. J. Membr. Sci. **107**(3), 229–237 (1995). https://doi.org/10.1016/0376-7388(95)00119-0
27. R.A. Hegab, S. Pardue, X. Shen, C. Kevil, N.A. Peppas, M.E. Caldorera-Moore, Effect of network mesh size and swelling to the drug delivery from pH responsive hydrogels. J. Appl. Polym. Sci. **137**(25), 48767 (2020). https://doi.org/10.1002/app.48767
28. D. Tian, J. Hu, J. Bao, R.P. Chandra, J.N. Saddler, C. Lu, Lignin valorization: lignin nanoparticles as high-value bio-additive for multifunctional nanocomposites. Biotechnol. Biofuels **10**(1), 192 (2017). https://doi.org/10.1186/s13068-017-0876-z